Vol 15 No 8, August 2006
1009-1963/2006/15(08)/1849-06

Chinese Physics

© 2006 Chin. Phys. Soc.
and IOP Publishing Ltd

Study on the delamination of tungsten thin films on Sb_2Te_3*

Xu Jia-Qing(徐嘉庆)[a)†], Liu Bo(刘 波)[a)], Song Zhi-Tang(宋志棠)[a)], Feng Song-Lin(封松林)[a)], and Chen Bomy[b)]

[a)] *Laboratory of Nanotechnology, Shanghai Institute of Microsystem and Information Technology, Chinese Academy of Science, Changning Road, Shanghai* 200050, *China*

[b)] *Silicon Storage Technology, Inc.*, 1171 *Sonora Court, Sunnyvale, CA* 94086, *USA*

(Received 25 August 2005; revised manuscript received 29 April 2006)

To investigate the reliability of electrode materials for chalcogenide random access memory (C-RAM) applications, the geometry and time evolution of the worm-like delamination patterns on a tungsten/Sb_2Te_3 bilayer system surface are observed by field emission scanning electronic microscope (FESEM) and optical microscopy. The tungsten film stress and interface toughness are estimated using a straight-side model. After confirming the instability of this system being due to large compressive stress stored in the tungsten film and relative poor interface adhesion, a preliminary solution as the inset of a TiN adhesion layer is presented to improve the system performances.

Keywords: C-RAM, delamination, adhesion
PACC: 4620, 4630, 7360D, 7360F

1. Introduction

In 1968, Ovshinsky discovered a new order–disorder memory phenomenon in Te-based chalcogenide glass.[1] Since then, this kind of material has aroused much interest of all due to the wide technical applications especially in optical phase-change data storage technology[2−4] and electrical nonvolatile memory devices, known as chalcogenide random access memory (C-RAM).[5−10] As a kind of resistance memory, the latter is required to have an electric layer in perfect and direct contact with the chalcogenide to introduce operating current. Especially, a top electrode is needed in two kinds of device structures (see Fig.1). Thus, a conductive layer should be deposited directly on the chalcogenide layer. On the other hand, tungsten is widely used in the solid electronic devices and circuits as an electrode material due to its thermal stability, good step coverage and high conductivity.

However, the delamination and cracking[11] of the compressed thin films is one of the greatest limitations on structural performances. The film buckles from the interface to relieve strain energy, and the delamination patterns are treated as a result of the competition and balance between the compressive stresses within the film and its adhesion to the underlayer. If the adhesion is strong, a perfect contact is kept. When it is overwhelmed by the compressive stress, the system becomes unstable and delamination or spalling occurs to release the stored strain energy. Several kinds of delamination patterns, such as straight-sided column, worm-like and varicose shapes[12−16] are observed or predicted. In this paper, the tungsten/ Sb_2Te_3 (a chalcogenide material in the widely investigated GeTe-Sb_2Te_3 pseudobinary system in the phase-change data storage technology[5]) system is investigated experimentally in order to provide some evidence for C-RAM device manufacture.

*Project Supported by the National High Technology Development Program of China (Grant No 2004AA302G20), Science and Technology Council of Shanghai (Grant Nos 0452nm012, 04DZ05612, 04ZR14154, 04JC14080, 05JC14076, AM0414, 05nm05043, AM0517), Chinese Academy of Sciences (Grant No Y2005027), and Silicon Storage Technology, Inc.

†Corresponding author, E-mail: xjq@mail.sim.ac.cn

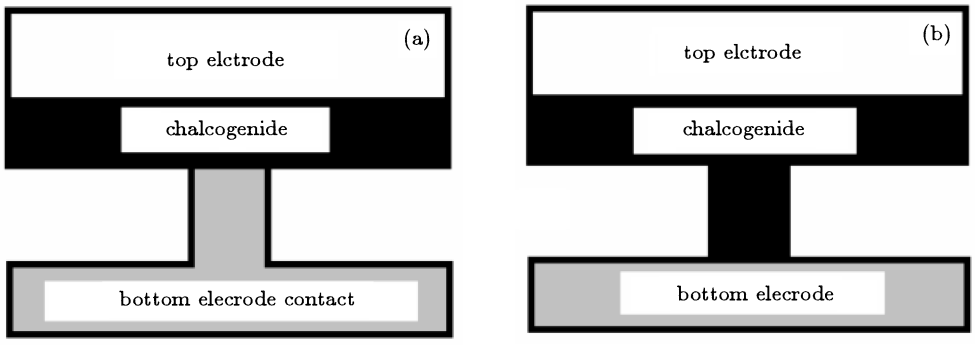


Fig.1. The schematics of two possible device structures.

2. Experiments

RF magnetron sputtering is employed to deposit 50-nm amorphous Sb_2Te_3 thin films on Si (100)/SiO_2 substrates using a Sb_2Te_3 target. W films with a thickness ranging from 5 to 100 nm are then deposited on the chalcogenide. The Ar pressure during sputtering is 0.2 Pa and the sputtering power is in a range of 100–300 W. The TiN film is deposited by reactively sputtering a Ti target in the mixture of N_2 and Ar with a N_2/Ar ratio of 1. Field emission scanning electronic microscope (FESEM, HITACHI S4700) and optical microscopy are then used to observe the delamination patterns.

3. Pattern geometry and its original sites

Typical optical images of the oriented worm-like (or telephone cord) patterns on the film surface are shown in Fig.2. The patterns here are formed by using the W film separated from the Sb_2Te_3 layer. As shown in Fig.3, the FESEM cross section of the sample whose top view is displayed in Fig.2(a) indicates that the 50-nm Sb_2Te_3 layer adheres to the substrate perfectly but the 75-nm W film humps up. To our knowledge, the delamination of tungsten /chalcogenide system is reported for the first time. The underlying Sb_2Te_3 layer here promotes the delamination of the W film because no buckling is observed for such a thin W film on Si (100)/SiO_2.

In Fig.2, two samples respectively with 75-nm W on 50-nm Sb_2Te_3 and with 50-nm W on 50-nm Sb_2Te_3 are photographed about one hour later after the deposition. Similar patterns are observed for those with a W film thickness of above 25nm. The width of the wavy lines increases with the film thickness, which is coincident with the results of the carbon film.[17,18]

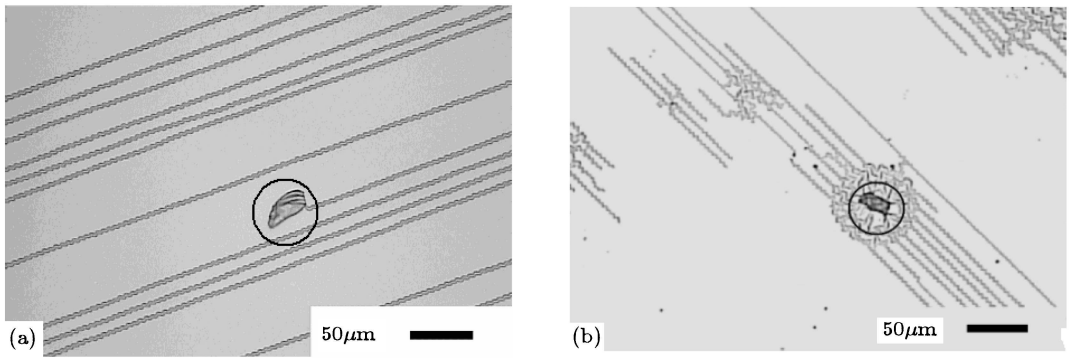


Fig.2. Optical images of two samples respectively with (a) 75-nm W on 50-nm Sb_2Te_3 and (b) with 50-nm W on 50-nm Sb_2Te_3.

However, 5- and 15-nm W films remain well bonded to the underlayer even when they have been exposed to the air for several days. As discussed by Lee *et al*,[19] the strain energy stored in the thin film increases with the increase of film thickness before reaching a maximum and it decreases in a thicker film.

So the unbuckled W films are assumed to stay in the pre-maximum domain where the strain energy is not large enough to overwhelm the adhesion.

The wavy lines on an as-deposited film usually originate from the contaminated sites on the substrate surface (see the circled site in Fig.2(b)) or the imperfections along the substrate edge. As suggested by Evans *et al*[20] and Yu *et al*,[21] the delamination of such an interface requires a pre-existent separation. The contaminated sites and the edge defects can act as the source of such initial separations during the deposition. Early study has shown that a certain number of the sources of this kind are required to generate a substantial delamination.[20] Thus, the compressive stress around the edge of the initial circular separation should exceed a critical value

$$\sigma_{\rm c} = 1.215E/(1-\nu^2)\ (h/a)^2, \tag{1}$$

where a is the radius of separation, h is the thickness of film, ν is its Poisson ratio and E is Young's modulus. When the film forms under compression, the delamination propagates starting from all initial separations ($h \to 0$). However, only larger separations can induce buckling when the thickness increases. From the viewpoint of the system stored energy, in recent experiments[19,22] a more general and practical parameter energy release rate (or crack extension force) G, which means the total energy released per unit area of the film on the separation edge, of the initial separation is used to depict the delamination process related to the imperfections. G is usually expressed as a function of the geometry of the initial separation. When it exceeds the fracture toughness of the interface $\Gamma_{\rm int}$ (adhesion energy per unit area for the well-bonded film), the putative buckle will become unstable and propagate out of the imperfection until G on the new edge meets $\Gamma_{\rm int}$. Under this frame, Moon *et al*[22] classify the imperfect sites into three categories. For our experiments, the patterns in Fig.2(b) should be induced by 'super-critical' sites (the origin of well-defined patterns) within the circled areas, and the circled site in Fig.2(a) terminating the wavy line is assumed to be the 'sub-critical' one with little interface separation.

Although the wavy patterns always originate from the contaminated sites and the edge imperfections, the sources do not determine the pattern shape, which is the intrinsic characteristic of the bilayer system. For example, the wavelength is reported to be directly related to the intrinsic strain ε.[14,16]

4. Estimation of film stress and interface toughness from the pattern geometry

As mentioned above, pattern shape is an intrinsic characteristic of the bilayer system. It results from the very well-defined combination of internal stress, Young's modulus, film thickness and adhesion energy. Several models have been developed to estimate the mechanic properties of the film from the pattern geometry.[13,17,18] Although the observed wavy line propagates in a certain direction (see the next section for details), its side edge always stays stationary, which is modelled by straight-sided and pinned circular patterns.[18] The former method simply measures the cross-sectioned profile of the wavy lines at a straight portion and applies a set of equations to depicting the straight-sided blisters, while the latter considers the curved edges and involves numerically integrating the von Karman equations. Here we take a more concise straight-sided method to estimate the internal stress σ in the W film and the energy release rate G on the pattern's side edge (i.e. the fracture toughness of the interface $\Gamma_{\rm int}$ in a steady state as mentioned in Section 3). The results obtained from this method and also from the alleged more accurate pinned circular method are proved to be in good agreement with each other in a large stress case.[18,19]

Assume that the W thin film with a thickness h is subject to equi-biaxial compression σ, and the cross-sectioned profile of the wavy lines will have the form

$$w = w_{\rm max}/2(1+\cos(\pi y/b)), \tag{2}$$

where w is the surface displacement of the delaminated W layer normal to the substrate at the parallel-substrate direction coordinate y, $2b$ is the profile width with a maximum height being

$$w_{\rm max} = h(4/3(\sigma/\sigma_{\rm c}-1))^{1/2}. \tag{3}$$

The critical stress $\sigma_{\rm c}$ for the straight-sided case is

$$\sigma_{\rm c} = \pi^2/12(E/(1-\nu^2))\ (h/b)^2. \tag{4}$$

The fracture toughness of the W/Sb_2Te_3 interface, $\Gamma_{\rm int}$, is given by

$$\Gamma_{\rm int} = G = G_0(1-\sigma_{\rm c}/\sigma)(1+3\sigma_{\rm c}/\sigma), \tag{5}$$

where

$$G_0 = (1-\nu^2)h\sigma^2/(2E) \tag{6}$$

is the stored strain energy per unit area in the W film.

The internal stress σ is calculated from Eq.(3), while Eq.(5) gives the $\Gamma_{\rm int}$. Poisson's ratio ν and Young's modulus E of W are taken as 0.28 and 40 Gpa respectively. For the 75-nm W sample, b is measured under the optical microscope to be $2\,\mu$m, and $w_{\rm max}$ is estimated to be 400 nm from Fig.3 (there is no obvious deviation of $w_{\rm max}$ after being sectioned from that in Fig.7 in Ref.[21]). So the calculated internal stress σ is 1.12 GPa that is in the order of the internal stress for the W film deposited under a similar condition on the Si substrate measured by a cantilever beam technique.[23] The W/Sb_2Te_3 interface fracture toughness $\Gamma_{\rm int}$ is $1.17\,{\rm J/m^2}$, and the toughness is assumed by the straight-side model to be a full toughness in shear mode[18] despite the successful simulation of the wavy patterns without considering this mode.[14,16] No further calculation of the different W thickness samples is undertaken here due to the accuracy limitation in our pattern geometry measurements where it is hard to provide comparable b and $w_{\rm max}$.

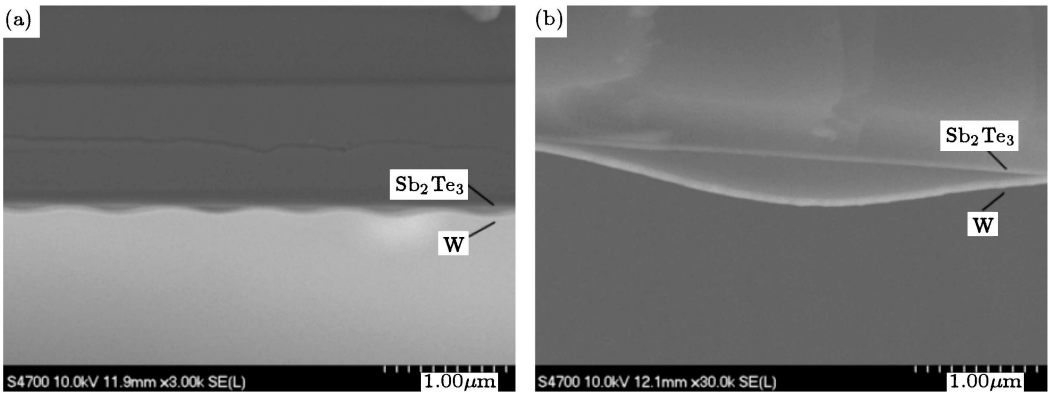


Fig.3. Cross section of (a) six parallel lines (b) one line on the surface of the sample shown in Fig.2(a).

5. Time evolution and instability of the bilayer system

As discussed in the previous section, both sides of the wavy patterns are in equilibrium. However, at the circular front of the delaminated line, the interface toughness stays in an open mode[18] and the wavy lines propagate further. The wriggling of the worm lines has ever been observed under optical microscope. The time evolution of the system is investigated below.

As soon as the as-deposited film is taken from vacuum to the atmosphere,[16] the wavy patterns start to form from imperfections and then propagate. When the samples are exposed to the air further, a considerable number of new wavy lines form in the pre-flat area induced by some initial separations. Although the sides of existing lines stay in equilibrium, the line boundary branches off (see Fig.4). This phenomenon assumably results from the toughness (adhesion) fluctuation around the side edge. When the branches are connected with the adjacent lines, a wrinkled network formes. For the thinner W samples (see Fig.4(b)) the early periodic wavy lines could hardly be identified. The patterns will cover the whole film surface and remain unchanged after a certain time. The length of the patterns depends on the film thickness. Although it is very sensitive to the initial contaminations on the substrate, the relaxation time increases with the decrease of W film thickness, ranging from several hours to a few days when the W film thickness decreases from 100 to 25 nm.

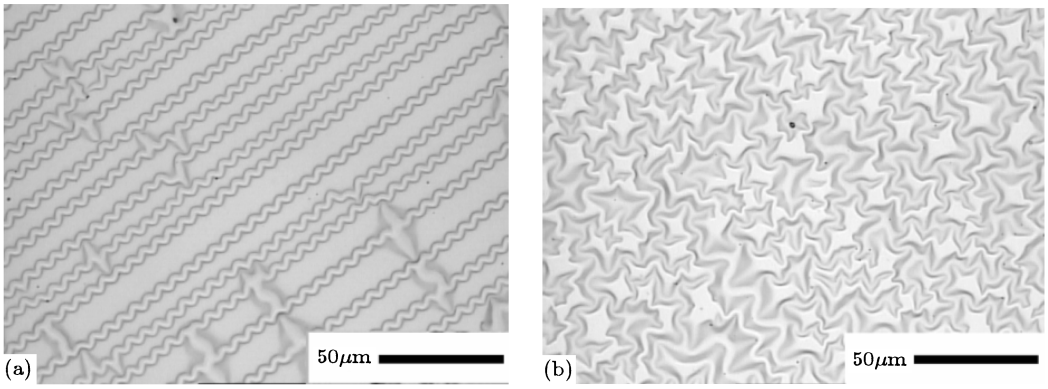


Fig.4. The final patterns of the corresponding samples shown in Fig.2.

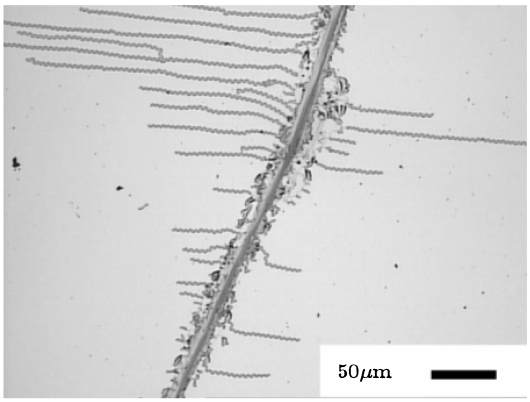


Fig.5. The scratching induced wavy lines on a 40-nm W / 50-nm Sb_2Te_3 sample.

The time evolution of the delamination patterns reveals the instability of the bilayer system existing. This system is also disturbed when its surface is scratched. As shown in Fig.5, arrays of wavy lines resulting from the scratching cause the separations to branch off.

6. A preliminary solution

An apparent solution of the delamination is to reduce the stored strain energy in the electrode layer or to improve the interface adhesion. A TiN layer that

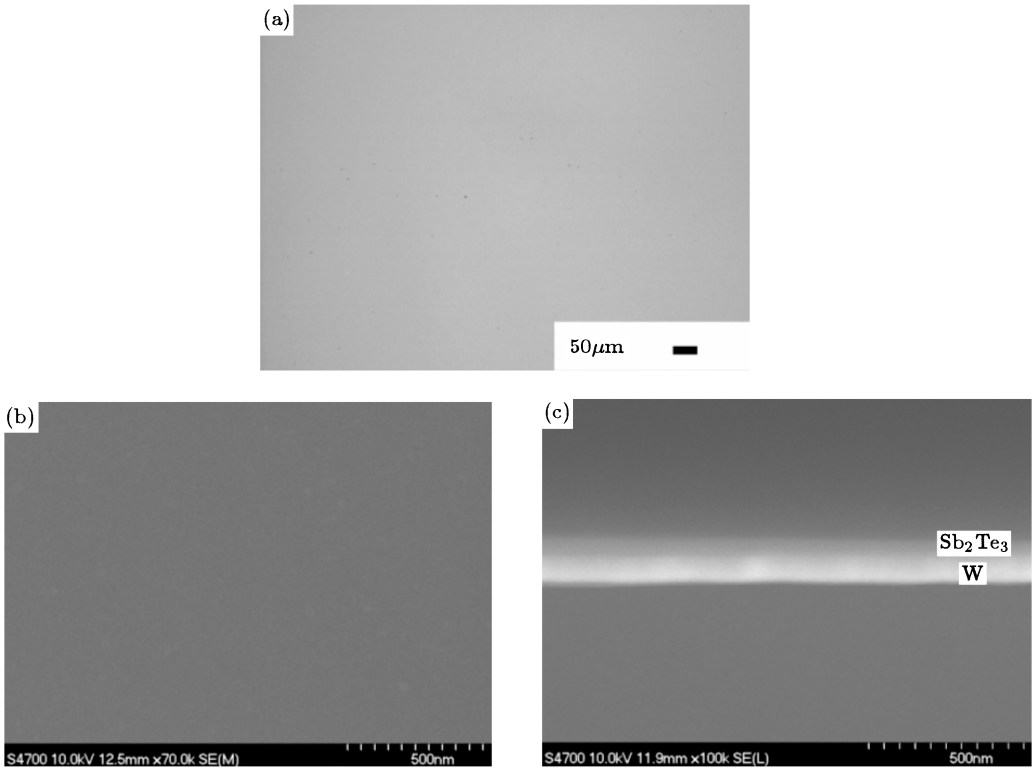


Fig.6. Top view of the 100-nm W / 10-nm TiN / 50-nm Sb_2Te_3 system surface by optical microscopy (a) and by FESEM (b). (c) is for cross section of the well-bonded film stack; the TiN layer is sandwiched between W and Sb_2Te_3 layers but it is too thin to be identified.

is widely applied has been used to try conglutinating W and Sb_2Te_3 layers. For a W film thickness ranging from 50 to 150 nm, the RF sputtered TiN layer is observed well bonding to both upper and underlying materials except for some substrate contaminations. Typical top view and cross-section of a tri-layer system (Sb_2Te_3(50nm)/ TiN(10nm)/ W(100nm)) are shown in Fig.6. The film surface is very smooth and W film bonds well to the underlying layer. No delamination is induced even after scratching the surface. So it is assumed that the film stack bears minor disturbances and stays in a relatively stable state. The mechanical and electrical measurements of the system will be carried out in the future for its optimization.

7. Summary

The W film on the Sb_2Te_3 layer shows that it stores relatively large strain energy and has a poor adhesion. The topography of the bilayer system is very sensitive to the initial contaminations on the substrate and the separations induced by scratching. These imperfections act as the source of the propagating wavy patterns formed by delaminated W film on Sb_2Te_3 underlayer. Therefore, the perfect contact is hard to accomplish in the W/Sb_2Te_3 system, which is required for introducing current in the C-RAM application. An adhesive TiN layer has been used as an inset under the W electrode and the propagating wavy patterns no longer exist. The W film with a thickness up to 100 nm also bonds well to the underlying Sb_2Te_3 film.

Acknowledgment

The authors would like to thank Miss Zheng Ming-Jie and Mrs Qian Rong for their help in FESEM and optical microscope observations.

References

[1] Ovshinsky S R 1968 *Phys. Rev. Lett.* **21** 1450
[2] Ohta T, Nishiuchi T, Narumi K, Kitaoka Y, Ishibashi H, Yamada N and Kozaki T 2000 *Jpn. J. Appl. Phys.* **39** 770
[3] Liu B, Ruan H and Gan F X 2003 *Chin. Phys.* **12** 107
[4] Liu B, Ruan H and Gan F X 2002 *Chin. Phys.* **11** 293
[5] Liu B, Song Z T, Feng S L and Chen B 2005 *Microelec. Engin.* **82** 168
[6] Liu B, Song Z T, Zhang T, Feng S L and Chen B 2004 *Chin. Phys.* **13** 1947
[7] Liu B, Song Z T, Zhang T, Feng S L and Gan F X 2004 *Chin. Phys.* **13** 1167
[8] Liu B, Song Z T, Feng S L and Chen B 2004 *Chin. Phys. Lett.* **21** 1143
[9] Liu B, Song Z T, Zhang T, Xia J L, Feng S L and Chen B 2005 *Thin Solid Films* **478** 49
[10] Liu B, Song Z T, Feng S L and Chen B 2005 *Chin. Phys. Lett.* **22** 758
[11] Ding H Z, Zhao R B and Xing X S 1996 *Chin. Phys.* **5** 1
[12] Nir D 1984 *Thin Solid Films* **112** 41
[13] Gille G and Rau B 1984 *Thin Solid Films* **120** 109
[14] Crosby K M and Bradley R M 1999 *Phys. Rev.* E **59** R2542
[15] Audoly B 1999 *Phys. Rev. Lett.* **83** 4124
[16] Peyla P 2000 *Phys. Rev.* E **62** R1501
[17] Matuda N, Baba S and Kinbara A 1981 *Thin Solid Films* **81** 301
[18] Moon M W, Jensen H W, Hutchinson J W, Oh K H and Evans A G 2002 *J. Mech. Phys. Solids* **50** 2355
[19] Lee A, Clemens B M and Nix W D 2004 *Acta Mater.* **52** 2081
[20] Evans A G and Hutchinson J W 1984 *Int. J. Solids Struct.* **20** 455
[21] Yu H Y, Kim C and Sanday S C 1991 *Thin Solid Films* **196** 229
[22] Moon M W, Chung J W, Lee K R, Oh K H, Wang R and Evans A G 2002 *Acta Mater.* **50** 1219
[23] Shen Y G, Mai Y W, Zhang Q C, McKenzie D R, McFall W D and McBride W E 2000 *J. Appl. Phys.* **87** 177